Scientia Psychiatrica
Vol. 7, No. 4, 2026, pp. 191–202 · e-ISSN 2715-9736 journal homepage: scientiapsychiatrica.com

ORIGINAL RESEARCH ARTICLE

Cross-Species Transcriptomic Analysis Finds No Global Reversal of Major Depressive Disorder Signatures by Luteolin

Nur Diana[1], Indri Yani Septiana[2], Annisa Annisa[3*]
[1]*Department of Molecular Biology, CMHC Research Center, Palembang, Indonesia*
[2]*Department of Physiology, CMHC Research Center, Palembang, Indonesia*
[3]*Department of Health Sciences, Baloi Medical Center, Batam, Indonesia*

ARTICLE INFO

Article history
Received: August 20, 2026
Revised: September 18, 2026
Accepted: October 19, 2026
Available online: October 27, 2026
Published: October 30, 2026

Keywords
Cross-species analysis
Luteolin
Major depressive disorder
Meta-analysis
Transcriptomic reversal

***Corresponding author**
Annisa Annisa
E-mail: annisa@gmail.com
ORCID: 0009-0001-9109-2427

DOI
10.37275/scipsy.v7i4.221

ABSTRACT

Background. Luteolin is active in experimental systems. Whether its transcriptional effects reverse those of major depressive disorder (MDD) is unknown.

Objective. To test whether luteolin responses in lipopolysaccharide-exposed systems reverse postmortem dorsolateral prefrontal cortex MDD signatures, and to identify gene- or pathway-level opposition for validation.

Methods. We reanalyzed three luteolin datasets (mouse hippocampus, GSE181285; human neural stem cells, GSE181522; mouse microglia, GSE18740) and two human MDD cohorts (GSE101521 and GSE54568). Technical replicates were aggregated by biological unit. Probes were collapsed independently of outcome. Mouse genes were restricted to one-to-one human orthologs, and effects were combined by random-effects meta-analysis. The primary endpoint was the Spearman correlation between luteolin rescue and MDD effects. We added bootstrap, permutation, distance-to-control, sensitivity, and Reactome analyses.

Results. Across 13,034 shared genes, rescue and MDD effects were weakly and positively correlated ($\rho = 0.041$, $p < 0.001$; bootstrap 95% CI 0.023–0.059; permutation $p = 0.001$). Reversal would have required a negative correlation. Of 302 genes nominally associated in both analyses, 143 (47.35%) were opposed ($p = 0.388$). Only neural stem cells moved closer to control. Excluding that dataset strengthened the positive correlation ($\rho = 0.074$); adding MDD-suicide cases weakened it ($\rho = 0.004$, $p = 0.685$). No Reactome pathway survived false-discovery-rate correction. Aerobic respiration and electron transport ranked first ($q = 0.058$).

Conclusion. The integrated evidence does not support global reversal of human MDD transcriptomic signatures by luteolin. Bioenergetic, oxidative, PKA–CREB, glutamatergic, and immune candidates remain targets for hypothesis generation. They need prospective, cell-resolved validation.

Copyright: © 2026 The Author(s). Published by HM Publisher in collaboration with CMHC Research Center on behalf of Scientia Psychiatrica. The authors retain copyright of their work.

Access licence: This is an open access article distributed under the terms of the Creative Commons Attribution–NonCommercial–ShareAlike 4.0 International Licence (CC BY-NC-SA 4.0), which permits non-commercial use, sharing, adaptation and reproduction in any medium, provided the original author and source are credited and any derivative work is distributed under the same licence.

1. Introduction

Major depressive disorder (MDD) is not a single molecular entity. It is a clinically and biologically heterogeneous syndrome. Recent studies of the human brain at cell resolution, together with systems-biological, metabolic, chromatin-accessibility, and multiomic work, have implicated distinct neuronal and non-neuronal programs, and they also show that bulk-tissue averages can hide cell-specific abnormalities, which a single averaged profile would never reveal.[1–5] The direction and cellular location of these signals shift with brain region, sex, phenotype definition, medication exposure, and analytic scale. Broad normalization claims are therefore hard to evaluate. Explicit tests of the direction, magnitude, and robustness of cross-study molecular concordance become more valuable.

Luteolin is a dietary flavone with pleiotropic antioxidant and immunomodulatory actions. In lipopolysaccharide (LPS)-exposed neural stem-cell models and in animal models related to depression, it has been linked to altered cell fate, microglial polarization, inflammatory signaling, endoplasmic-reticulum stress, synaptic plasticity, and JAK2/STAT3 activity.[6–10] Newer studies add effects on glycerophospholipid metabolism, stress-related behavior, oxidative and neurotrophic processes, BDNF signaling, and proteomic or protein-network candidates in depression-related settings.[11–16] Such

findings make luteolin a reasonable subject for neuroinflammatory models. They stop short of showing that it corrects the molecular state of the depressed human brain, and they say nothing about clinical efficacy, dosing, safety, or substitution for existing treatment. That gap is the subject here.

Transcriptomic signature reversal offers a stringent test of that translational claim. An intervention is expected to move a large shared gene set in the direction opposite to the disease signature. Connectivity-score comparisons, cell-specific imputation, and the L1000 Connectivity Map show what the approach can do and how strongly its answer depends on the chosen signature, model, and aggregation method.[17–19] A strong response inside an experimental system is not enough. The response must also run in the predicted negative direction against the target disease signature. Crossing species adds difficulty. One-to-one orthology does not guarantee equivalent regulation, and acute LPS exposure is not a full model of chronic MDD. Whole hippocampus, isolated neural stem cells, cultured microglia, and postmortem dorsolateral prefrontal cortex (DLPFC) also differ greatly in cell composition and basal state. Recent single-nucleus DLPFC, patient-derived GABA-interneuron, imaging–transcriptomic, and suicide-phenotype studies reinforce the weight of cell context and phenotype definition.[20–23] These sources of heterogeneity should be modeled or tested as sensitivities, never used to pick only the concordant results.

The present study integrates three experimental luteolin datasets with two human DLPFC MDD cohorts in a common effect-size framework. It separates four related but non-equivalent questions. Does luteolin have a measurable transcriptional effect? Is the combined LPS + luteolin condition closer to control than LPS alone? Do gene-level rescue effects oppose human MDD effects? Does any opposition concentrate in interpretable pathways? Keeping these questions apart stops large experimental effects from being misread as disease reversal, and it lets a negative global result coexist with narrower mechanistic signals that deserve a separate look.

This study provides an uncertainty-aware cross-species test of luteolin against a meta-analyzed human MDD transcriptomic target. The test preserves biological units, adds an independent phenotype-definition sensitivity analysis, and triangulates rank concordance with distance, gene-opposition, and pathway endpoints. Our primary aim was simple. We asked whether the meta-analytic luteolin rescue signature correlates negatively with human DLPFC MDD effects. Secondarily, we sought reproducible gene or pathway opposition that could be validated prospectively.

2. Methods

2.1. Study design and setting

Study design and reporting. This was a secondary integrative analysis of publicly available transcriptomic data. The prespecified conceptual contrast was the effect of luteolin in an inflammatory context, defined as LPS plus luteolin versus LPS, compared with the disease effect of MDD versus unaffected control in human DLPFC. The analysis was organized around biological units rather than array counts, retained effect direction and standard errors, and used multiple complementary endpoints. Reporting was adapted from the STROBE statement[24] for transparent description of observational secondary-data components, supplemented by explicit reporting of experimental contrasts, cross-species mapping, and reproducibility checks.

2.2. Participants

Data sources and analytic populations. Five Gene Expression Omnibus series were included. The accession-level systems, contrasts, and analytic-unit counts are detailed in Table 1. GSE181285 contained mouse hippocampal profiles across control, LPS, luteolin, and LPS + luteolin groups. Its 16 arrays represented eight mice because each mouse had two technical replicates; the replicates were averaged before modeling, leaving two biological units per group. GSE181522 contained seven human neural stem-cell arrays across corresponding experimental conditions, including a single control array. GSE18740 contained 12 mouse microglial arrays, with three arrays per group. These datasets directly supported an LPS-context luteolin contrast and provided gene-level expression data. The very small hippocampal groups and single neural stem-cell control were treated as design constraints rather than expanded through technical observations. The sample sizes were fixed by the deposited datasets, and no a priori sample-size calculation was applicable.

The primary human disease target combined GSE101521 and GSE54568. In GSE101521, complete cases were required for age, sex, RNA integrity number, postmortem interval, brain pH, and diagnostic variables. The primary contrast included 28 controls and nine MDD cases whose recorded cause-of-death category did not indicate suicide. Twenty-one MDD-suicide cases were reserved for sensitivity analysis. GSE54568 contributed 30 samples in 15 matched control–MDD pairs, and the pairing factor was retained.

Table 1. Data sources, contrasts, and analytic units.

Accession and system	Species	Analytic units	Role and contrast
GSE181285; hippocampus	Mouse	16 arrays from 8 mice; 2 mice per group	Luteolin rescue: (LPS + luteolin) − LPS
GSE181522; neural stem cells	Human	7 arrays; control n = 1	Luteolin rescue: (LPS + luteolin) − LPS
GSE18740; microglia	Mouse	12 arrays; 3/group	Luteolin rescue: (LPS + luteolin) − LPS
GSE101521; DLPFC	Human	28 controls; 9 MDD; 21 MDD-suicide in sensitivity	MDD − control; adjusted complete-case model
GSE54568; DLPFC	Human	30 samples; 15 matched pairs	MDD − control; pair-adjusted model

DLPFC, dorsolateral prefrontal cortex; LPS, lipopolysaccharide; MDD, major depressive disorder; GSE, Gene Expression Omnibus series.

2.3. Variables and instruments

Expression preprocessing and gene annotation. GEO Series Matrix files and platform annotations were parsed programmatically. Values were inspected to determine whether $\log_2$ transformation was required. Quantile normalization was applied where the source scale and distribution warranted it; depositor-provided normalized counts for GSE101521 were retained after scale checks Platform probes were mapped to gene symbols. When several probes mapped to the same gene, the probe with the highest interquartile range (IQR) was selected using expression variability alone, avoiding selection based on diagnosis or treatment outcome.

For GSE101521, Ensembl identifiers were linked to gene symbols using the NCBI gene-to-Ensembl mapping used in the analysis archive. Mouse genes were mapped to human symbols through Mouse Genome Informatics homology groups and retained only when a group contained exactly one mouse and one human symbol. This conservative restriction reduced ambiguity from paralogous mappings. All integration steps were conducted in the resulting human-symbol space, and the intersection of genes available in the luteolin and MDD meta-analyses defined the primary test set.

2.4. Data collection procedure

Covariate handling and missing data. Covariate handling was deliberately cohort-specific. GSE101521 contained measured continuous tissue-quality and demographic variables that could be incorporated directly, whereas GSE54568 was designed around matched pairs and was analyzed through that pairing rather than by forcing an identical covariate set. Complete-case restriction was applied before the diagnostic model, and no values were imputed. The resulting estimates therefore target the available samples with measured covariates; they do not represent all deposited cases. Diagnosis coefficients were oriented consistently as MDD minus control, and rescue coefficients as (LPS + luteolin) minus LPS, so a negative cross-gene association had an unambiguous interpretation.

2.5. Statistical analysis

Differential-expression models. Within each luteolin dataset, linear models estimated four contrasts: LPS versus control, LPS + luteolin versus LPS (the rescue effect), the combined condition versus control, and the interaction [(LPS + luteolin) − LPS] − [luteolin − control]. Limma moderated statistics stabilized variance estimates in small transcriptomic studies.[25] The hippocampal model used mouse-level averages; the neural stem-cell and microglial models used the available arrays as stated in their source designs. Results were expressed as $\log_2$-scale effects, standard errors, nominal p values, and Benjamini–Hochberg false-discovery-rate (FDR) values.

For GSE101521, the MDD non-suicide versus control model adjusted for age, sex, RNA integrity number, postmortem interval, and brain pH. For GSE54568, the diagnostic contrast included the matched-pair factor. A sensitivity model for GSE101521 expanded the MDD group to include the 21 MDD-suicide cases while retaining the same measured covariates. The human models estimated tissue-level associations; they were not interpreted as causal disease effects because of the postmortem observational design.

Gene-level meta-analysis. The three rescue effects were combined separately for each gene by inverse-variance random-effects meta-analysis. Between-study variance (τ^2) was estimated using the DerSimonian–Laird method, and Cochran Q and I^2 were retained as descriptive heterogeneity measures. The two human MDD effects were combined in a second random-effects meta-analysis. With only two or three studies per gene, estimates of between-study heterogeneity are imprecise; therefore, the pooled effect, its standard error, direction across datasets, and sensitivity results were interpreted together rather than treating I^2 as a stable biological parameter.

Primary transcriptomic reversal endpoint. The primary endpoint was Spearman rank correlation between the random-effects luteolin rescue beta and the random-effects MDD beta across all shared genes. Global transcriptomic reversal required $\rho < 0$. A two-sided asymptotic p value was reported, but the sign and magnitude of ρ were the primary interpretive quantities. Uncertainty was estimated with 2,000 gene-level bootstrap samples. An empirical two-sided p value was obtained from 999 permutations that disrupted the pairing between rescue and MDD gene labels.

Genes are organized in correlated pathways, so neither gene bootstrap nor label permutation creates independent biological replication. These procedures quantify stability of the observed genome-wide pairing under the stated analytic universe; they do not replace replication across independent organisms, cultures, or patient cohorts. Accordingly, statistical significance for a very small ρ was not interpreted as practical evidence of reversal. The scripted analysis was rerun

independently, and a validation script checked the primary ρ, nominal overlap counts, opposition counts, and number of FDR-significant pathways.

Distance-to-control analysis. Within each experimental dataset, a standardized root-mean-square distance was calculated as D = RMS[(LPS + luteolin) − control] / RMS[LPS − control]. A ratio below 1 indicated movement toward control; a ratio above 1 indicated movement away from control. Gene-bootstrap 95% intervals summarized stability across the measured transcriptome. Because the resampled elements were genes, narrow intervals were not taken to imply precise biological-unit effects, particularly in datasets with two mice per group or one control array.

Gene opposition and pathway analysis. A descriptive gene subset required nominal $p < 0.05$ for both the rescue and MDD meta-analytic effects. The proportion with opposite beta signs was compared with 50% using an exact binomial test. For broader prioritization, an opposition score integrated effect magnitude and opposite direction across the full shared-gene set. The top 5% of ranked genes were tested for over-representation in Reactome pathways using a one-sided Fisher exact test, with all mapped shared genes as the universe, pathway sizes restricted to 15–500 genes, and Benjamini–Hochberg correction. Reactome definitions corresponded to the 2022 knowledgebase.[26] Because the 5% threshold was a ranking convention and genes within pathways are correlated, pathway results were designated exploratory, with FDR < 0.05 required for confirmatory language.

Sensitivity analyses and software. Two sensitivity analyses addressed prominent design choices. First, the neural stem-cell dataset was removed from the rescue meta-analysis because its control group contained a single array. Second, MDD-suicide cases were added to the GSE101521 disease contrast to examine dependence on phenotype definition. The complete analysis was executed in R using scripted preprocessing, limma modeling, random-effects pooling, resampling, and figure generation. Exact package and platform versions are documented in the archived R session-information file. The rerun reproduced the archived summaries, and the independent validation returned PASS.

Reproducibility. Analytic decisions were fixed across the independent rerun. The biological-unit aggregation, highest-IQR probe rule, one-to-one ortholog filter, model matrices, gene universe, resampling counts, and pathway-size restrictions were not altered after the new output was inspected. Quality checks reconciled accession identifiers, group counts, complete matched pairs, and non-empty figure and table products. The validation script recalculated the primary rank correlation and confirmed 302 genes meeting both nominal thresholds, 143 opposed genes, and zero Reactome pathways at q < 0.05. This addresses computational reproducibility. Biological reproducibility is a separate question that only independent experiments can answer.

2.6. Ethical approval

Ethical approval was granted by the CMHC Research Center Ethics Committee Indonesia (No. 2026/028). Consent and ethics procedures for the original human tissue studies were governed by the respective primary-study protocols.

3. Results

3.1. Sample reconciliation and mapped transcriptome

The experimental source files comprised 35 arrays: 16 hippocampal, seven neural stem-cell, and 12 microglial. Aggregating the two technical replicates per mouse in GSE181285 gave 27 experimental analytic units across the three studies. The primary human component held 67 samples, namely 37 complete-case GSE101521 samples and 30 samples from 15 matched GSE54568 pairs. After one-to-one ortholog mapping, the cross-species intersection contained 13,034 genes.

The transcriptomic response varied sharply by system. GSE181285 yielded no FDR-significant genes for LPS versus control, rescue, or interaction, which fits its limited biological replication. GSE181522 yielded thousands of FDR-significant genes, although its single control array made the scale of these differential results particularly dependent on that one culture. In GSE18740, 379 genes were FDR-significant for LPS versus control and 19 for the rescue contrast; this was the most replicated dataset-specific evidence of a luteolin-associated response. The human random-effects MDD meta-analysis yielded 1,399 genes at nominal $p < 0.05$. Of these, 10 reached FDR < 0.05.

3.2. Movement toward the experimental control state

Table 2 gives the complete endpoint estimates, and Figure 1 shows the three distance ratios. In GSE181285, the LPS + luteolin centroid lay farther from control than the LPS centroid (ratio 1.369, gene-bootstrap 95% CI 1.345–1.393). GSE181522 moved toward control (0.900, 0.891–0.909). GSE18740 moved slightly away from it (1.049, 1.039–1.059). Only one of three systems therefore met the prespecified directional criterion, and that system had the least informative control replication.

Table 2. Primary, supporting, and sensitivity endpoints.

Endpoint	Estimate	Interpretation
Primary rescue–MDD rank correlation	ρ = 0.041; 95% CI 0.023–0.059; p < 0.001	Positive; does not meet reversal criterion
Permutation test	p = 0.001; 999 permutations	Positive pairing; unlikely under label permutation
Nominally informative genes	143/302 opposed; p = 0.388	No excess above 50%
GSE181285 distance ratio	1.369 (1.345–1.393)	Away from control
GSE181522 distance ratio	0.900 (0.891–0.909)	Toward control
GSE18740 distance ratio	1.049 (1.039–1.059)	Away from control
Exclude neural stem cells	ρ = 0.074; p < 0.001	Positive; no reversal
Include MDD-suicide cases	ρ = 0.004; p = 0.685	Approximately null

CI, confidence interval; LPS, lipopolysaccharide; MDD, major depressive disorder; ρ, Spearman rank correlation.

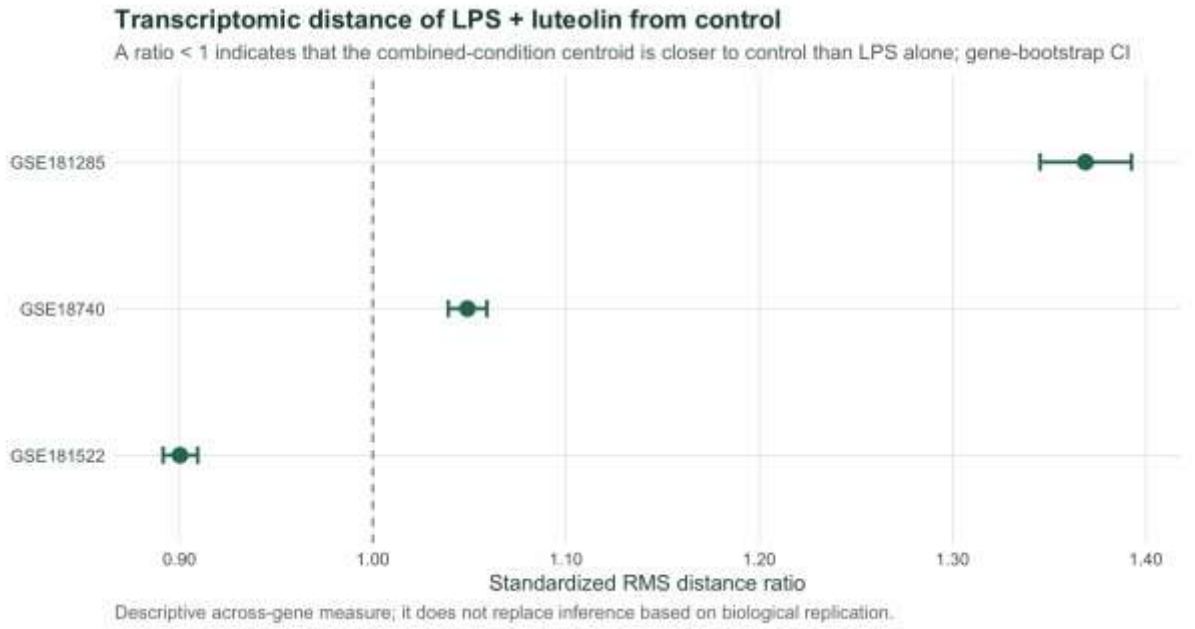


Figure 1. Transcriptomic distance to control in each luteolin experiment. The ratio is D = RMS[(LPS + luteolin) − control] / RMS[LPS − control]. Values below 1 indicate movement toward control; values above 1 indicate movement away. Error bars are gene-bootstrap 95% intervals and do not substitute for biological-unit replication. CI, confidence interval; LPS, lipopolysaccharide; RMS, root mean square.

3.3. Primary cross-species reversal test

Rescue and MDD meta-analytic effects were available for 13,034 shared genes. Their Spearman correlation was ρ = 0.0409 (asymptotic p = 3.05×10^{-6}), with a 2,000-bootstrap 95% CI from 0.023 to 0.059 and a 999-permutation p = 0.001. Figure 2 shows the paired cross-gene effects. The large number of genes made this small association statistically detectable. Yet the correlation was positive, not negative, and its magnitude was close to zero. It failed the direction required for global transcriptomic reversal, and it described little shared rank structure.

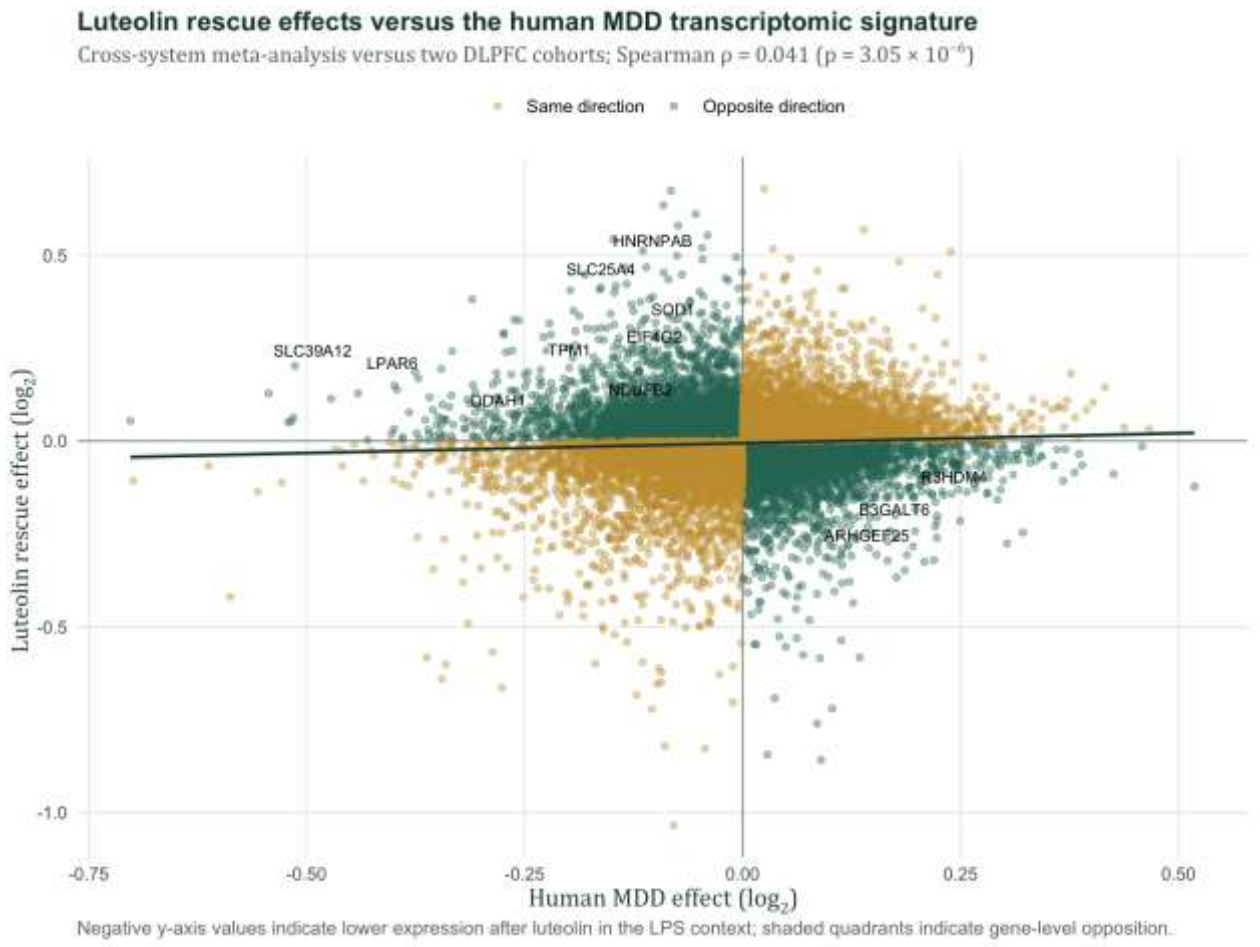


Figure 2. Cross-species transcriptomic reversal test across 13,034 shared genes. Each point pairs the random-effects luteolin rescue estimate [(LPS + luteolin) minus LPS] with the random-effects human MDD estimate (MDD minus control). Global reversal required a negative association; the observed Spearman correlation was small and positive (ρ = 0.041). DLPFC, dorsolateral prefrontal cortex; LPS, lipopolysaccharide; MDD, major depressive disorder. Orange points, same direction; green points, opposite direction.

Among 302 genes with nominal $p < 0.05$ in both meta-analyses, 143 had opposite signs (47.35%). That proportion did not exceed the 50% reference expectation (exact binomial $p = 0.388$). The global rank endpoint, the nominal-overlap endpoint, and the distance analysis converged on the same result: no broad normalization. The conclusion did not depend on requiring genome-wide significance within the small individual experiments.

3.4. Sensitivity to experimental and human phenotype definitions

Removing the neural stem-cell dataset left 12,885 shared genes and raised the positive rescue–MDD correlation to $\rho = 0.074$ ($p = 3.21 \times 10^{-17}$). The poorly replicated neural stem-cell control was therefore unlikely to explain the failure to observe reversal. In the second sensitivity analysis, adding the 21 MDD-suicide cases to GSE101521 weakened the primary correlation to $\rho = 0.004$ ($p = 0.685$). Neither analysis produced a negative correlation. One estimate became more positive once neural stem cells were excluded, and the other was approximately null once the human phenotype was broadened. This contrast suggests that the small positive primary association was not a universal property of luteolin or MDD.

3.5. Opposed genes and pathway signals

Several highly ranked opposed genes tied rescue effects to cellular energetics, redox regulation, translation, lipid/immune signaling, and nitric-oxide metabolism. Examples included HNRNPAB, SOD1, SLC25A4, EIF4G2, LPAR6, DDAH1, B3GALT6, ARHGEF25, R3HDM4, SLC39A12, NDUFB2, and TPM1. Figure 3 gives their dataset-level and pooled estimates Many had precise rescue effects but uncertain MDD effects. HNRNPAB, for example, showed a large and highly precise positive rescue estimate but only a small negative MDD estimate with $q > 0.05$. These ranks identify experimental candidates, not validated MDD biomarkers.

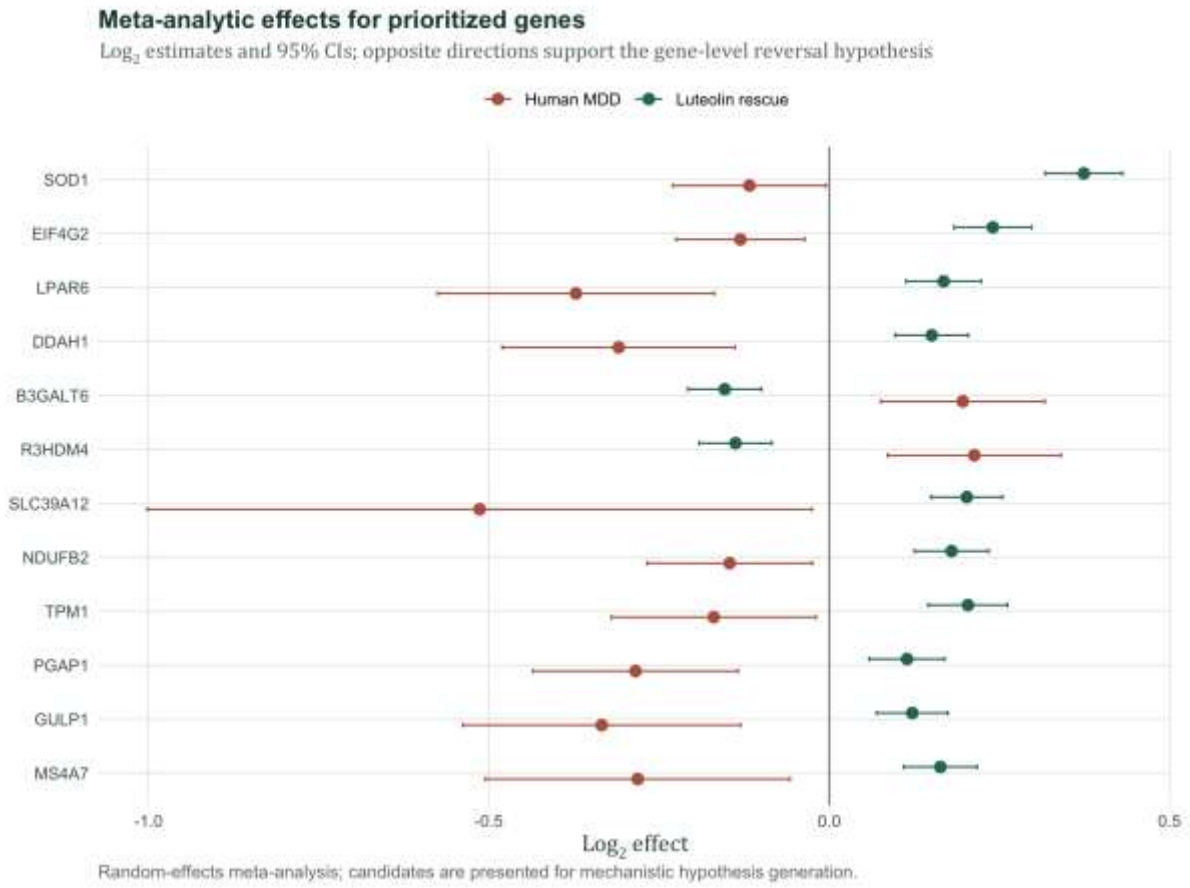


Figure 3. Dataset-level and meta-analytic effects for prioritized opposed genes. The display separates the precision of the experimental luteolin contrast from the human MDD estimate and shows when a pooled rank is driven by a subset of systems. Candidates are hypothesis-generating and are not validated biomarkers. CI, confidence interval; MDD, major depressive disorder. Red, human MDD estimate; green, luteolin rescue estimate.

No Reactome pathway passed FDR < 0.05. Table 3 lists the leading enrichment results. Aerobic respiration and respiratory electron transport contained 23 prioritized genes (odds ratio 2.80, $p = 4.51 \times 10^{-5}$, q = 0.058), and respiratory electron transport ranked next (15 genes; odds ratio 2.95; $p = 5.15 \times 10^{-4}$; q = 0.333). Smaller nominal signals included complex I biogenesis, PKA activation, PKA-mediated phosphorylation of CREB, and FCGR3A-mediated interleukin-10 synthesis, but their corrected values did not support pathway-level claims. The pattern was good enough to guide assays. It was not enough to establish a mechanism.

Table 3. Leading Reactome over-representation results among the top 5% opposed genes.

Pathway	Overlap	OR	p; q
Aerobic respiration and respiratory electron transport	23	2.80	<0.001; 0.058
Respiratory electron transport	15	2.95	<0.001; 0.333
Complex I biogenesis	7	3.37	0.008; 1.000
FCGR3A-mediated IL-10 synthesis	6	4.12	0.006; 1.000
PKA activation	4	6.39	0.007; 1.000
PKA-mediated phosphorylation of CREB	4	5.90	0.009; 1.000

OR, odds ratio. One-sided Fisher exact tests used the 13,034-gene shared universe; q values are Benjamini–Hochberg adjusted. No pathway met q < 0.05.

4. Discussion

4.1. Principal findings

This cross-species analysis found no evidence that luteolin globally reverses the transcriptomic state associated with human MDD. The result is more than a nonsignificant test. The genome-wide correlation was statistically detectable but weakly positive, and reversal required a negative one. Two further endpoints agreed: fewer than half of the genes nominally associated with both signatures were opposed, and only one of three experimental systems moved closer to its control state, while sensitivity analyses revealed no hidden negative relationship. Taken together, these findings separate a measurable biological response to luteolin from normalization of a human disease signature.

4.2. Comparison with the existing literature

The distinction matters because pharmacologic activity and disease reversal answer different questions. Luteolin altered many transcripts in neural stem cells

and a smaller replicated set in microglia, in line with earlier evidence of neurogenic and immunomodulatory actions.[6,7] A compound can nevertheless have large effects that are unrelated, orthogonal, or even parallel to a disease-associated contrast. Connectivity-map studies show the value of direction-based prioritization, and they also show that reversal metrics are sensitive to the disease signature, the model context, and the aggregation method.[17–19] The present result narrows the translational claim. It leaves the experimental biology intact.

4.3. Interpretation and mechanism

Biological interpretation of the absent global reversal. This is useful mainly as a model-selection result. A simple narrative would have LPS produce a depression-like transcriptome and luteolin return it toward a healthy human state, and that narrative predicts agreement across the rank, distance, and directional-overlap endpoints. It did not hold. Only the neural stem-cell system moved toward its experimental control, and the cross-species rank relationship stayed nonnegative under both sensitivities. The data are compatible with a context-dependent model, which this analysis did not test directly. In it, luteolin engages selected cellular programs, and the relation of those programs to the average human MDD signature varies with tissue, cell state, and phenotype definition, which yields narrower, testable predictions and avoids treating every transcriptional change as therapeutic correction.

Several mechanisms could explain why LPS-context luteolin responses did not oppose bulk DLPFC MDD effects. Acute LPS exposure emphasizes innate immune signaling. MDD, by contrast, develops through heterogeneous combinations of genetic liability, stress exposure, endocrine signaling, synaptic adaptation, metabolism, vascular biology, and treatment history. Recent studies of circulating myeloid MMP8, astrocyte-mediated neutrophil recruitment, and blood–brain-barrier biology show that inflammatory and vascular mechanisms can matter without forming a single universal disease state.[27–29] Reversing an acute inflammatory state is neither necessary nor sufficient for reversing the average postmortem MDD transcriptome.

The tissues also differ in cellular makeup. Whole hippocampus mixes neurons, glia, vascular cells, and infiltrating immune signals. Cultured microglia and neural stem cells isolate particular states, whereas bulk DLPFC averages several cortical layers and cell types after death. Experimental work links microglial PCGF1, astrocytic pleiotrophin, microglial circ-UBE2K, complement-dependent synapse pruning, ERK–NRBP1–CREB–BDNF signaling, and astrocyte autophagy to stress- or depression-related phenotypes.[30–35] A true cell-specific effect could thus be diluted, or even counterbalanced in direction, in bulk tissue. The reverse can also occur, because an apparent bulk opposition might reflect shifting cell proportions rather than within-cell correction.

Sex and phenotype definition add more heterogeneity. Cell-resolved depression studies report both shared and sex-linked patterns, and including suicide deaths changes the clinical and agonal makeup of a cohort.[1,23] Adding MDD-suicide cases in our sensitivity analysis lowered ρ from 0.041 to 0.004. This does not prove that suicide status causes the difference, because cause of death covaries with unmeasured exposures and tissue conditions. It does show that the disease target is not invariant. Any claim of treatment reversal should name the human signature it targets.

Bioenergetic and oxidative candidates. The leading pathway and several opposed genes converged on mitochondrial and redox biology. Aerobic respiration and electron transport approached the 5% FDR threshold without crossing it, and SOD1, SLC25A4, and NDUFB2 were among the notable opposed genes. Human iPSC-derived neural models, patient-derived neural progenitors and neurons, multiomic analyses, and stress-model experiments involving TAMM41, Hippo/YAP signaling, NDUFB9, and mitophagy have each tied mitochondrial biology to depression-related phenotypes.[36–42] This outside support raises the priority of the module for validation. It does not turn q = 0.058 into a positive pathway finding.

The best follow-up would test whether luteolin changes mitochondrial respiration, ATP production, reactive oxygen species, and complex I function in independent donor-derived cells, while measuring the corresponding transcripts and proteins. A mechanistic claim would need a consistent direction across batches, a dose–time relationship, perturbation of a candidate mediator, and rescue of a prespecified cellular phenotype. Candidate selection should favor genes supported in more than one luteolin system and stable across both MDD cohorts. Genes that rank highly only because of one extreme estimate from a single experiment should not be favored.

PKA–CREB, glutamatergic, and immune hypotheses. Nominal pathway ranks also linked PKA–CREB signaling, glutamatergic receptor biology, and FCGR3A-mediated interleukin-10 synthesis. These processes offer reasonable bridges between inflammatory signaling, synaptic plasticity, and neural-cell state. Recent circuit experiments show excitation–inhibition imbalance in depression-related states and roles for parvalbumin- and cholecystokinin-expressing GABAergic neurons, and human brain organoids tie antidepressant exposure to electrophysiology and metabolic reprogramming.[43–45] Yet the relevant Reactome pathways had high q values and small overlaps. They should guide a compact, prespecified assay panel. They do not support a narrative that these pathways were restored.

The gene-level results show why precision on one side of the comparison is not enough. Several candidates had very small rescue q values but uncertain human MDD estimates. This asymmetry reflects the strength of the experimental response in particular datasets and the heterogeneity of postmortem disease effects. A translational candidate should ideally combine four

things. It needs a reproducible intervention effect, a stable disease-direction estimate, compatible cell-type expression, and a functional endpoint, all supported by more than one dataset. The current ranking meets only part of that chain.

4.4. Implications for practice and policy

Statistical and practical importance. Candidate prioritization should therefore be two-dimensional. The first dimension is intervention credibility: replication across independent luteolin systems, a moderate pooled effect not driven by a single study, and functional confirmation at the protein or metabolic level. The second is disease relevance: directionally consistent effects in both DLPFC cohorts, localization to an implicated cell population, and association with a prespecified human phenotype. HNRNPAB shows why a strong rescue estimate alone falls short. Mitochondrial candidates gain interest from pathway convergence and outside bioenergetic evidence. Even for these, the right output of this study is an assay shortlist, not a biomarker panel.

The primary ρ illustrates the gap between statistical and practical importance. With more than 13,000 genes, a correlation near 0.04 can give a small p value. Squaring the coefficient is not a formal variance decomposition for ranks, but it conveys how little ordering the two signatures share. It is small. The sign matters more, and it contradicted the hypothesis. Reporting only $p = 3.05 \times 10^{-6}$ would invert the scientific meaning of the result. The bootstrap and permutation analyses showed that the small positive ordering was stable under gene resampling and label disruption. They did not show that it was a beneficial reversal.

Distance-to-control intervals were narrow for the same kind of reason: genes, not animals or independent cultures, were resampled. Biological precision remains limited by two mice per hippocampal group and one neural stem-cell control. The distances are useful as descriptive whole-transcriptome geometry, but they cannot replace confidence intervals built on adequately replicated experimental units. The modest movement away from control in microglia does not rule out improvement in a subset of inflammatory genes. Equally, movement toward control in neural stem cells cannot establish general rescue.

Clinical or practical importance cannot be inferred from transcriptomic geometry alone. A molecular signature may lie downstream of disease, be compensatory, or be unrelated to symptoms. A compound may also influence behavior through mechanisms that leave the measured tissue signature untouched. Conversely, molecular opposition without adequate exposure at the target tissue would not produce a treatment effect. This analysis contains no pharmacokinetic, toxicologic, symptom, relapse, or comparative-treatment data. Its practical contribution is modest. It prevents overextension of a broad reversal claim and directs resources toward experiments that can link molecular target engagement to functional outcomes.

Implications and future research. The evidence supports a conditional mechanistic program, not a global reversal claim. Independent neural stem-cell, microglial, and neuron-containing systems should be studied with at least three biological batches, balanced controls, prespecified doses and time points, and blinded outcome measurement. Candidate mitochondrial, redox, PKA–CREB, glutamatergic, and interleukin-10 measures should be paired with respiration, ATP, reactive-oxygen-species, synaptic, and cytokine endpoints. Genetic or pharmacologic perturbation can then test whether candidate genes mediate the luteolin response or merely accompany it. Correlation alone will not settle that.

Later stages should use induced pluripotent stem-cell models from independent MDD and control donors, followed by cell-resolved animal experiments that include both sexes and hippocampal and prefrontal regions. One human disease signature, reversal metric, gene universe, ortholog rule, and pathway procedure should be preregistered before the validation data are examined. Clinical studies would be justified only after pharmacokinetic and toxicologic evidence, and they should begin with safety and target-engagement endpoints, not assumed antidepressant efficacy. Recent postmortem single-nucleus and bulk-expression work shows how shared and diagnosis-specific abnormalities can be separated in future human validation.[46]

A decisive validation sequence would start with balanced, donor-replicated cell experiments and reserve one independent dataset for a locked analysis. The primary molecular endpoint should be a signed correlation against one prespecified human signature, reported with biological-unit uncertainty. Secondary endpoints should cover distance to control, a fixed candidate panel, and a pathway method that accounts for gene correlation. Advancement should require concordant molecular and functional effects at realistic exposure. Nominal pathway enrichment alone would not suffice. A future positive reversal result could then be read as replicated target engagement, with mechanistic evidence kept distinct from clinical benefit.

4.5. Strengths and limitations

Strengths. The study has several strengths. It uses open, accession-specific data and a fully scripted pipeline. Technical hippocampal replicates were aggregated before inference, so the same mouse could not contribute duplicate biological degrees of freedom. Matched pairs were preserved in GSE54568, and measured tissue-quality covariates were included in GSE101521. The integration kept signed effect estimates and their standard errors instead of comparing arbitrary significant-gene lists. Several endpoints tested the same core claim, and prominent design limitations were examined through sensitivity analyses. The key numerical outputs were reproduced in an independent rerun and checked with a validation script.

Limitations. The experimental evidence is limited by small biological samples, particularly two mice per

hippocampal group and one neural stem-cell control. Arrays in culture studies may not correspond to independent donors, which constrains generalization beyond the sampled cultures, whereas the microglial experiment had better group replication but represented one isolated cell system. The large number of significant genes in the neural stem-cell dataset should be read as a strong contrast within that experiment. It is not a precise population estimate.

The analysis also combined species, platforms, tissues, and perturbation schedules. Restricting integration to one-to-one orthologs reduced mapping ambiguity but did not ensure equivalent regulation. Quantile normalization and within-platform modeling supported comparable effect direction, yet cross-platform beta magnitudes are not perfectly exchangeable. Random-effects models accommodated heterogeneity. With two or three studies, however, τ^2 and I^2 are unstable. Postmortem MDD effects remain open to residual medication, comorbidity, agonal, cell-composition, and technical influences, despite covariate adjustment and matching.

Gene-level bootstrap and permutation analyses treated genes as resampling units, although coexpression makes them dependent. Their intervals and empirical probabilities are best understood as transcriptome-level stability summaries. The top-5% opposition threshold and the over-representation analysis were exploratory, and no pathway survived FDR correction. Study selection rested on direct biological relevance and data availability, not on a systematic review of every luteolin experiment, so selection bias is possible. Finally, transcriptomic opposition is a surrogate concept. Even a strong negative correlation would not establish behavioral efficacy, human bioavailability, safety, or clinical benefit.

The human target is also an average across individuals. Depression subgroups with inflammatory, metabolic, or particular cell-state features could show relationships that the pooled DLPFC signature hides. Testing this requires individual-level molecular subtyping or a priori stratification; selecting responsive subgroups after seeing treatment effects would not do. Sex-stratified analyses could not be estimated with adequate precision across all component datasets, although sex can reverse the direction of depression-associated expression. The pooled result is thus evidence against a broad average reversal. It is not proof that every biologically defined subgroup lacks a luteolin-responsive mechanism.

5. Conclusion

Across 13,034 one-to-one orthologous genes, luteolin rescue effects in three LPS-context experimental systems were not negatively correlated with human DLPFC MDD effects. The correlation was small. It was also positive. Nominally overlapping genes were not enriched for opposite direction. Two of three systems did not move closer to control, and no Reactome pathway passed FDR correction, so the evidence does not support global transcriptomic reversal of MDD by luteolin.

This conclusion is compatible with biologically meaningful, context-dependent luteolin activity. The mitochondrial, oxidative, PKA–CREB, glutamatergic, and immune candidates give a focused agenda for prospective validation. They are not evidence of clinical antidepressant efficacy. Therapeutic inferences must wait. They require balanced biological replication, cell-resolved models, prespecified analysis, functional perturbation, and human target-engagement data.

Declarations

Use of Generative Artificial Intelligence. None. The authors declare that no generative artificial intelligence tool was used in the conception, research, analysis, drafting, revision or preparation of this manuscript.

Author Contributions. N.D.: conceptualization, methodology, software, formal analysis, data curation, visualization, writing – original draft. I.Y.S.: validation, investigation, writing – review & editing. A.A.: supervision, project administration, writing – review & editing. All authors have read and approved the final version of the manuscript.

Funding. This work received no specific grant from any funding agency in the public, commercial, or not-for-profit sectors.

Conflict of Interest. The authors declare that they have no competing interests, financial or non-financial, in relation to this work.

Ethical Approval. Ethical approval was granted by the CMHC Research Center Ethics Committee Indonesia (No. 028/CMHC/Ethics/09/2026).

Informed Consent. Not applicable to the present secondary analysis. Consent and ethics procedures for the original human tissue studies were governed by the respective primary-study protocols.

Data Availability. All expression data are publicly available from the NCBI Gene Expression Omnibus under GSE181285, GSE181522, GSE18740, GSE101521, and GSE54568. The analysis scripts, provenance manifest, quality-control records, tables, and figures are available from the corresponding author on reasonable request.

Acknowledgements. None.

References

1. Maitra M, Mitsuhashi H, Rahimian R, et al. Cell type specific transcriptomic differences in depression show similar patterns between males and females but implicate distinct cell types and genes. Nat Commun. 2023;14(1):2912. doi:10.1038/s41467-023-38530-5
2. Daskalakis NP, Iatrou A, Chatzinakos C, et al. Systems biology dissection of PTSD and MDD across brain regions, cell types, and blood. Science. 2024;384(6698):eadh3707. doi:10.1126/science.adh3707
3. Li XY, Rao Y, Li GH, et al. Single-nucleus RNA sequencing uncovers metabolic dysregulation in the prefrontal cortex of major depressive disorder patients. Sci Rep. 2025;15(1):7418. doi:10.1038/s41598-025-92030-8
4. Chawla A, Cakmakci D, Fiori LM, et al. Single-nucleus chromatin accessibility profiling identifies cell types and functional variants contributing to major depression. Nat

Genet. 2025;57(8):1890-1904. doi:10.1038/s41588-025-02249-4

5. Francis A, Dwivedi Y. Multiomic single-nucleus profiling reveals cell-type-specific epigenetic and transcriptional dysregulation in major depressive disorder brain. Int J Neuropsychopharmacol. 2026:pyag045. doi:10.1093/ijnp/pyag045
6. Achour M, Ferdousi F, Sasaki K, et al. Luteolin modulates neural stem cells fate determination: in vitro study on human neural stem cells, and in vivo study on LPS-induced depression mice model. Front Cell Dev Biol. 2021;9:753279. doi:10.3389/fcell.2021.753279
7. Yuan NJ, Zhu WJ, Ma QY, et al. Luteolin ameliorates chronic stress-induced depressive-like behaviors in mice by promoting the Arginase-1+ microglial phenotype via a PPARγ-dependent mechanism. Acta Pharmacol Sin. 2025;46(3):575-591. doi:10.1038/s41401-024-01402-9
8. Tana, Nakagawa T. Luteolin ameliorates depression-like behaviors by suppressing ER stress in a mouse model of Alzheimer's disease. Biochem Biophys Res Commun. 2022;588:168-174. doi:10.1016/j.bbrc.2021.12.074
9. Cheng Y, Wang X, Yu Y, et al. Noise-induced depression-like behavior, neuroinflammation and synaptic plasticity impairments: the protective effects of luteolin. Neurochem Res. 2022;47(11):3318-3330. doi:10.1007/s11064-022-03683-0
10. Wu HH, Chen SY, Yuan DL, et al. Luteolin alleviates CUMS-induced depressive-like behavioral deficits in mice through blocking the JAK2/STAT3 pathway. PLoS One. 2025;20(10):e0335057. doi:10.1371/journal.pone.0335057
11. Wu X, Xu H, Zeng N, et al. Luteolin alleviates depression-like behavior by modulating glycerophospholipid metabolism in the hippocampus and prefrontal cortex of LOD rats. CNS Neurosci Ther. 2024;30(3):e14455. doi:10.1111/cns.14455
12. Sur B, Lee B. Luteolin reduces fear, anxiety, and depression in rats with post-traumatic stress disorder. Anim Cells Syst (Seoul). 2022;26(4):174-182. doi:10.1080/19768354.2022.2104925
13. Mokhtari T, Lu M, El-Kenawy AE. Potential anxiolytic and antidepressant-like effects of luteolin in a chronic constriction injury rat model of neuropathic pain: role of oxidative stress, neurotrophins, and inflammatory factors. Int Immunopharmacol. 2023;122:110520. doi:10.1016/j.intimp.2023.110520
14. Ryu D, Jee HJ, Kim SY, et al. Luteolin-7-O-glucuronide improves depression-like and stress coping behaviors in sleep deprivation stress model by activation of the BDNF signaling. Nutrients. 2022;14(16):3314. doi:10.3390/nu14163314
15. Liu K, Li H, Zeng N, et al. Exploration of the core pathways and potential targets of luteolin treatment on late-onset depression based on cerebrospinal fluid proteomics. Int J Mol Sci. 2023;24(4):3485. doi:10.3390/ijms24043485
16. Zhao T, Sun S, Gao Y, et al. Luteolin and triptolide: potential therapeutic compounds for post-stroke depression via protein STAT. Heliyon. 2023;9(8):e18622. doi:10.1016/j.heliyon.2023.e18622
17. Samart K, Tuyishime P, Krishnan A, et al. Reconciling multiple connectivity scores for drug repurposing. Brief Bioinform. 2021;22(6):bbab161. doi:10.1093/bib/bbab161
18. Sapashnik D, Newman R, Pietras CM, et al. Cell-specific imputation of drug connectivity mapping with incomplete data. PLoS One. 2023;18(2):e0278289. doi:10.1371/journal.pone.0278289
19. Subramanian A, Narayan R, Corsello SM, et al. A next generation Connectivity Map: L1000 platform and the first 1,000,000 profiles. Cell. 2017;171(6):1437-1452.e17. doi:10.1016/j.cell.2017.10.049
20. Chatzinakos C, Pernia CD, Morrison FG, et al. Single-nucleus transcriptome profiling of dorsolateral prefrontal cortex: mechanistic roles for neuronal gene expression, including the 17q21.31 locus, in PTSD stress response. Am J Psychiatry. 2023;180(10):739-754. doi:10.1176/appi.ajp.20220478
21. Lu K, Hong Y, Tao M, et al. Depressive patient-derived GABA interneurons reveal abnormal neural activity associated with HTR2C. EMBO Mol Med. 2023;15(1):e16364. doi:10.15252/emmm.202216364
22. Xia M, Liu J, Mechelli A, et al. Connectome gradient dysfunction in major depression and its association with gene expression profiles and treatment outcomes. Mol Psychiatry. 2022;27(3):1384-1393. doi:10.1038/s41380-022-01519-5
23. Qin K, Li H, Zhang H, et al. Transcriptional patterns of brain structural covariance network abnormalities associated with suicidal thoughts and behaviors in major depressive disorder. Biol Psychiatry. 2024;96(6):435-444. doi:10.1016/j.biopsych.2024.01.026
24. von Elm E, Altman DG, Egger M, et al. The Strengthening the Reporting of Observational Studies in Epidemiology (STROBE) statement: guidelines for reporting observational studies. Lancet. 2007;370(9596):1453-1457. doi:10.1016/S0140-6736(07)61602-X
25. Ritchie ME, Phipson B, Wu D, et al. Limma powers differential expression analyses for RNA-sequencing and microarray studies. Nucleic Acids Res. 2015;43(7):e47. doi:10.1093/nar/gkv007
26. Gillespie M, Jassal B, Stephan R, et al. The Reactome pathway knowledgebase 2022. Nucleic Acids Res. 2022;50(D1):D687-D692. doi:10.1093/nar/gkab1028
27. Cathomas F, Lin HY, Chan KL, et al. Circulating myeloid-derived MMP8 in stress susceptibility and depression. Nature. 2024;626(8001):1108-1115. doi:10.1038/s41586-023-07015-2
28. Yao H, Jiang SY, Jiao YY, et al. Astrocyte-derived CCL5-mediated CCR5+ neutrophil infiltration drives depression pathogenesis. Sci Adv. 2025;11(21):eadt6632. doi:10.1126/sciadv.adt6632
29. Dion-Albert L, Cadoret A, Doney E, et al. Vascular and blood-brain barrier-related changes underlie stress responses and resilience in female mice and depression in human tissue. Nat Commun. 2022;13(1):164. doi:10.1038/s41467-021-27604-x
30. Li N, Du J, Yang Y, et al. Microglial PCGF1 alleviates neuroinflammation-associated depressive behavior in adolescent mice. Mol Psychiatry. 2025;30(3):914-926. doi:10.1038/s41380-024-02714-2
31. Chi D, Zhang K, Zhang J, et al. Astrocytic pleiotrophin deficiency in the prefrontal cortex contributes to stress-induced depressive-like responses in male mice. Nat Commun. 2025;16(1):2528. doi:10.1038/s41467-025-57924-1
32. Cai Y, Ji Y, Liu Y, et al. Microglial circ-UBE2K exacerbates depression by regulating parental gene UBE2K via targeting HNRNPU. Theranostics. 2024;14(10):4058-4075. doi:10.7150/thno.96890
33. Hao W, Ma Q, Wang L, et al. Gut dysbiosis induces the development of depression-like behavior through abnormal synapse pruning in microglia mediated by complement C3. Microbiome. 2024;12(1):34. doi:10.1186/s40168-024-01756-6
34. Yao W, Cao Q, Luo S, et al. Microglial ERK–NRBP1–CREB–BDNF signaling in sustained antidepressant actions of (R)-ketamine. Mol Psychiatry. 2022;27(3):1618-1629. doi:10.1038/s41380-021-01377-7
35. He S, Shi Y, Ye J, et al. Does decreased autophagy and dysregulation of LC3A in astrocytes play a role in major depressive disorder? Transl Psychiatry. 2023;13(1):362. doi:10.1038/s41398-023-02665-2

36. Cardon I, Grobecker S, Jenne F, et al. Serotonin effects on human iPSC-derived neural cell functions: from mitochondria to depression. Mol Psychiatry. 2024;29(9):2689-2700. doi:10.1038/s41380-024-02538-0
37. Triebelhorn J, Cardon I, Kuffner K, et al. Induced neural progenitor cells and iPS-neurons from major depressive disorder patients show altered bioenergetics and electrophysiological properties. Mol Psychiatry. 2024;29(5):1217-1227. doi:10.1038/s41380-022-01660-1
38. Liao J, Wang X, Dai G, et al. Decoding nuclear-encoded mitochondrial genes in major depressive disorder: a multi-omics perspective. Psychol Med. 2025;55:e350. doi:10.1017/S0033291725102559
39. Guo L, Liu Z, Jia X, et al. Mitochondrial protein TAMM41 modulates depressive-like behaviors. Mol Neurobiol. 2024;61(12):10561-10573. doi:10.1007/s12035-024-04233-1
40. Zhao Y, Chen Y, Guo C, et al. Chronic stress dysregulates the Hippo/YAP/14-3-3η pathway and induces mitochondrial damage in basolateral amygdala in a mouse model of depression. Theranostics. 2024;14(9):3653-3673. doi:10.7150/thno.92676
41. Sun Y, Li L, Yang X, et al. NDUFB9 ameliorates CUMS-induced depression-like behavior by promoting mitophagy. Transl Psychiatry. 2025;15(1):292. doi:10.1038/s41398-025-03502-4
42. Han M, Xie B, Yu Y, et al. Intestinal γδ T17–IL-17A signaling disrupts hippocampal mitophagy in stress-induced depression and is restored by arketamine. J Neuroinflammation. 2025;23(1):24. doi:10.1186/s12974-025-03656-4
43. Tao C, Zhang GW, Sun WJ, et al. Excitation–inhibition imbalance in medial preoptic area circuits underlies chronic stress-induced depression-like states. Nat Commun. 2024;15(1):8575. doi:10.1038/s41467-024-52727-2
44. Asim M, Wang H, Waris A, et al. Basolateral amygdala parvalbumin and cholecystokinin-expressing GABAergic neurons modulate depressive and anxiety-like behaviors. Transl Psychiatry. 2024;14(1):418. doi:10.1038/s41398-024-03135-z
45. Li M, Duan W, Hao X, et al. Effects of esketamine on electrophysiology and metabolic reprogramming in brain organoids: insights into antidepressant mechanisms. Mol Psychiatry. 2025;30(12):6107-6118. doi:10.1038/s41380-025-03198-4
46. Gao R, Otsuka I, Shirai T, et al. Postmortem brain single-nucleus and bulk gene expression analyses identify shared and distinct abnormalities in bipolar disorder and major depressive disorder. Transl Psychiatry. 2026;16(1):442. doi:10.1038/s41398-026-04200-5